To be submitted to ApJL

Spectroscopic confirmation of a redshift 1.55 supernova host galaxy from the Subaru Deep Field Supernova Survey[1]

Teddy F. Frederiksen[1], Or Graur[2,3], Jens Hjorth[1], Dan Maoz[2], Dovi Poznanski[2]

teddy@dark-cosmology.dk

ABSTRACT

The Subaru Deep Field (SDF) Supernova Survey discovered 10 Type Ia supernovae (SNe Ia) in the redshift range $1.5 < z < 2.0$, as determined solely from photometric redshifts of the host galaxies. However, photometric redshifts might be biased, and the SN sample could be contaminated by active galactic nuclei (AGNs). Unfortunately, measuring spectroscopic redshifts of galaxies in the "redshift desert" $1.5 < z < 2.0$ is hard because any prominent emission lines get shifted out of the optical and into the near infrared. Here we report the first robust redshift measurement and classification of hSDF0705.25, an SDF SN Ia host galaxy. Using the X-shooter spectrograph on the Very Large Telescope, we measure a spectroscopic redshift of 1.5456 ± 0.0003, consistent with its photometric redshift of 1.552 ± 0.018. From the strong emission-line spectrum we are able to rule out AGN activity and show that the SN host galaxy is a low-metallicity, starbursting dwarf galaxy, similar to typical SN Ia hosts at lower redshifts. This represents a successful test case for the X-shooter spectrograph and shows that, though still hard, it is now possible to measure robust redshifts for SN host galaxies in the redshift desert.

Subject headings: galaxies: abundances — galaxies: distances and redshifts

---

[1]Dark Cosmology Centre, Niels Bohr Institute, University of Copenhagen, Juliane Maries Vej 30, 2100 Copenhagen, Denmark

[2]School of Physics and Astronomy, Tel-Aviv University, Tel-Aviv 69978, Israel

[3]Department of Astrophysics, American Museum of Natural History, Central Park West and 79th Street, New York, NY 10024-5192, USA

[1]Based on observations made with ESO telescopes at the La Silla Paranal Observatory under program ID 089.A-0739

1. INTRODUCTION

The nature of the progenitor stellar systems of type Ia supernovae (SNe Ia) remains a mystery (see Howell 2011 and Maoz & Mannucci 2012 for reviews). While both circumstantial and direct lines of evidence point to a carbon-oxygen white dwarf (WD; Nugent et al. 2011; Bloom et al. 2012 and see Leibundgut 2000 for a review) as the progenitor, the otherwise stable WD must be ignited. The current consensus is that the carbon in the core of the WD is ignited due to the buildup of pressure, or temperature, resulting from mass accretion from a companion star in a binary system. The two leading scenarios for the nature of the progenitor binary system are the single degenerate scenario (SD; Whelan & Iben 1973; Nomoto 1982), which contends that the WD accretes mass from a main-sequence, helium, or giant star; and the double degenerate scenario (DD; Iben & Tutukov 1984; Webbink 1984), in which the WD merges with a second CO WD through loss of angular momentum and energy to gravitational waves.

One way to discriminate between the SD and DD scenarios is through the delay-time distribution (DTD; the distribution of times that elapse between a short burst of star formation and the subsequent SN Ia explosions). Whereas most SD DTDs fall to zero after a few Gyr (though see, e.g., Di Stefano, Voss, & Claeys 2011; Hachisu, Kato, & Nomoto 2012), the DD DTD is a power law with index ~ -1, with power out to a Hubble Time. The SN Ia DTD has been recovered directly using different methods and SN samples (see Maoz & Mannucci 2012 for a review, and Maoz, Mannucci, & Brandt 2012; Graur & Maoz 2012 for subsequent studies). There are also indirect methods to recover the DTD. One such method relies on the measurement of volumetric SN Ia rates in field galaxies at cosmic time t, $R_{\rm Ia}(t)$. These SN Ia rates are the convolution of the cosmic star formation history (SFH), $S(t)$, with the DTD, $\Psi(t)$:

$$R_{\rm Ia}(t) = \int_0^t S(t-t')\Psi(t')dt'. \quad (1)$$

Thus, the DTD can be recovered by comparing the field SN Ia rates to the cosmic SFH at different redshifts.

Measurements of the volumetric SN Ia rate in field galaxies agree out to $z \sim 1$ [e.g., Perrett et al. 2012; Graur et al. 2011 (G11) and references therein]. These measurements were first extended to $z > 1$ by Dahlen et al. (2004), with additional data analyzed by Dahlen, Strolger, & Riess (2008), using the *Hubble Space Telescope* Advanced Camera for Surveys to survey the GOODS fields (Riess et al. 2004). Based on a sample of 3 SNe Ia at $z > 1.4$, they argued that the SN Ia rate declined at $z > 0.8$. Fitting this declining SN Ia rate evolution, Strolger et al. (2004) and Strolger, Dahlen, & Riess (2010) surmised that the DTD is confined to delay times of 3–4 Gyr. Conducting a similar SN survey in the Subaru

Deep Field (SDF) with the Subaru 8.2-m Telescope, G11 discovered 150 SNe, of which 28 (10) were $1 < z < 1.5$ ($z > 1.5$) SNe Ia. The G11 SN Ia rates indicate that the SN Ia rate evolution does not decline at high redshifts, but rather levels off, as predicted by the DD scenario.

However, the classification of the SNe discovered in the SDF is purely photometric and depends on the redshift of the host galaxy. As detailed below, the redshifts of most of the SDF SN host galaxies, including those at $z > 1.5$, are photometric redshifts (photo-z's). These photo-z's are based on photometry in 11 bands, from the far-ultraviolet (UV) to the near-infrared (IR), trained on hundreds of galaxies in the field with spectroscopy. Yet, because of the inherent difficulty in obtaining spectroscopic redshifts for early-type galaxies due to the lack of strong emission lines, training the photo-z method used by G11 in that range is difficult. There could be systematic biases in the redshift estimates in that bin, biases that are not accounted for in the formal uncertainty. Because of the small number of SN candidates, even a few 'catastrophic' photo-z failures could strongly distort the final results. While G11 used several methods to weed out interloping active galactic nucelei (AGNs), as each SN in the SDF sample was only observed in one epoch, there could still be some AGN contamination as well. In order to determine whether the G11 $z > 1.5$ rate suffers from such systematic biases, the host galaxies of the SN candidates must be observed spectroscopically, in order to measure their redshifts robustly, and to ascertain whether any of them harbor an AGN.

In this paper we present a VLT/X-shooter emission-line spectrum, derive the spectroscopic redshift and classify AGN vs. star-formation activity of the SN host galaxy hSDF0705.25. We also place constraints on the metallicity and star-formation rate of the host galaxy.

Throughout this paper we assume a flat ΛCDM cosmology with $H_0 = 70$ km s^{-1} and $\Omega_m = 0.3$.

2. DATA

2.1. Photometric Data

G11 derived SN host-galaxy photo-z's using the Zurich Extragalactic Bayesian Redshift Analyzer (ZEBRA[2]; Feldmann et al. 2006). Briefly, the host galaxies are first fit to the Benítez

[2]http://www.exp-astro.phys.ethz.ch/ZEBRA/

(2000) galaxy spectral energy distributions (based on galaxy spectra from Coleman, Wu, & Weedman 1996 for E/S0, Sbc, Scd, and Irr galaxies and Kinney et al. 1996 for two starbursting galaxies). The residuals of these fits are analyzed for systematic errors, which are then removed from the host galaxy photometry catalog. This catalog was composed of photometry in 11 bands, from the far-UV to the near-IR: far-UV (*FUV*) and near-UV (*NUV*) from the *Galaxy Evolution Explorer* (*GALEX*; Ly et al. 2009); *B*, *V*, *R*, i', z', *NB*816, and *NB*921 from the Subaru 8.2-m Telescope (Kashikawa et al. 2004); and *J* and *K*, where available, from the United Kingdom Infrared Telescope (Hayashi et al. 2009; Motohara et al., in preparation). Next, the basic galaxy templates are corrected using a training set of galaxies with known spectroscopic redshifts. G11 used a training set of 431 galaxies, of which 150 were in the range $1 < z < 2$ (see their section 4.2 for a detailed description). The resulting corrected templates are interpolated to produce a range of intermediate galaxy spectral templates. These templates are then used in an iterative Bayesian procedure, where the redshift and template probability distributions (PDFs) produced in each step are used as priors for the next one.

The resultant root-mean-square scatter between the spectroscopic and photometric redshifts of the G11 training set was $\sigma_{\Delta z}/(1+z_s) = 0.075$ (where $\Delta z = z_s - z_p$) in the range $0 < z_p < 2$, after rejecting six 4σ outliers. For the 24 G11 host galaxies with spectroscopic redshifts, the scatter was smaller: $\sigma_{\Delta z}/(1+z_s) = 0.044$, with no 4σ outliers. However, due to the dearth of spectroscopic redshifts at $z > 1.5$ (only 24, or $\sim 6\%$ of the training-set galaxies), there is a possible bias towards systematically higher values in the G11 $z > 1.5$ photo-z's.

Using the above method, the $i' = 24$ mag host galaxy of SNSDF0705.25, denoted hSDF0705.25, was typed as a Sbc galaxy with a sharp z-PDF that peaked at $z_p = 1.552 \pm 0.018$. In Figure 1 we show the photometry of hSDF0705.25, along with the best-fitting galaxy spectral-energy distribution and resultant z-PDF.

Each SN candidate in the SDF was observed in one of four independent epochs, in the *R*, i', and z' bands. Consequently, variable AGNs can be mistaken for SNe. G11 identified interloping AGNs using a catalog of known variable AGNs in the SDF (provided by T. Morokuma) and by culling SN candidates that appeared in more than one of the four survey epochs (see their section 3.1 for a detailed description). However, lacking spectroscopy, the possibility that some of the $z > 1.5$ SDF SNe Ia are in fact AGNs cannot be ruled out.

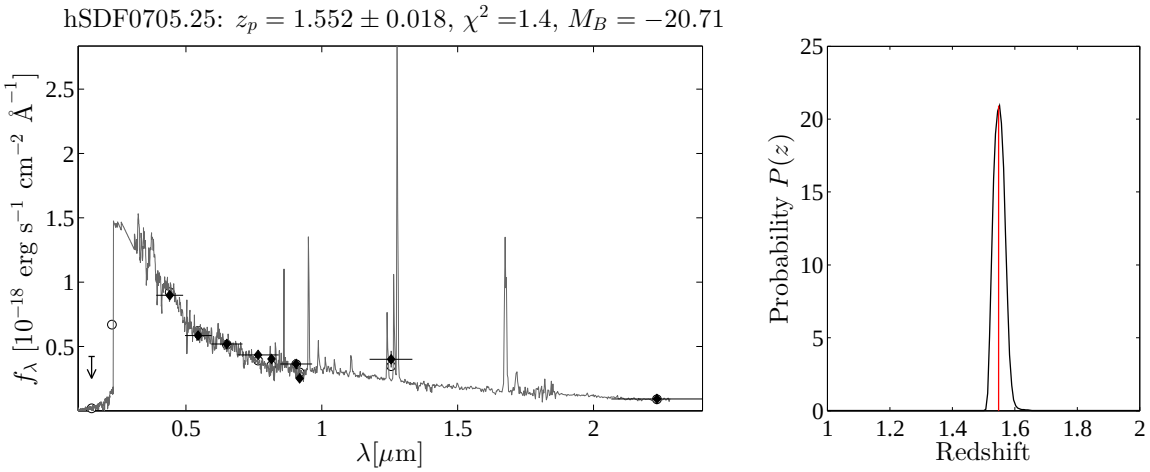

Fig. 1.— ZEBRA fit and resultant redshift PDF of hSDF0705.25. The left panel shows the actual photometry (filled circles), the best-fitting galaxy template (solid line), and its synthetic photometry (empty circles). The vertical error bars denote the photometric uncertainty, and the horizontal error bars show the width of the filter. The 1σ upper limit on the photometry in the *GALEX FUV* band is shown as the downturned arrow. The header gives the designation of the SN host galaxy, most probable photo-z (z_p), the χ^2 per degree of freedom of the fit, and the absolute B-band magnitude the object would have at z_p. The right panel shows the resultant z-PDF. The red line marks the spectroscopic redshift obtained in this work.

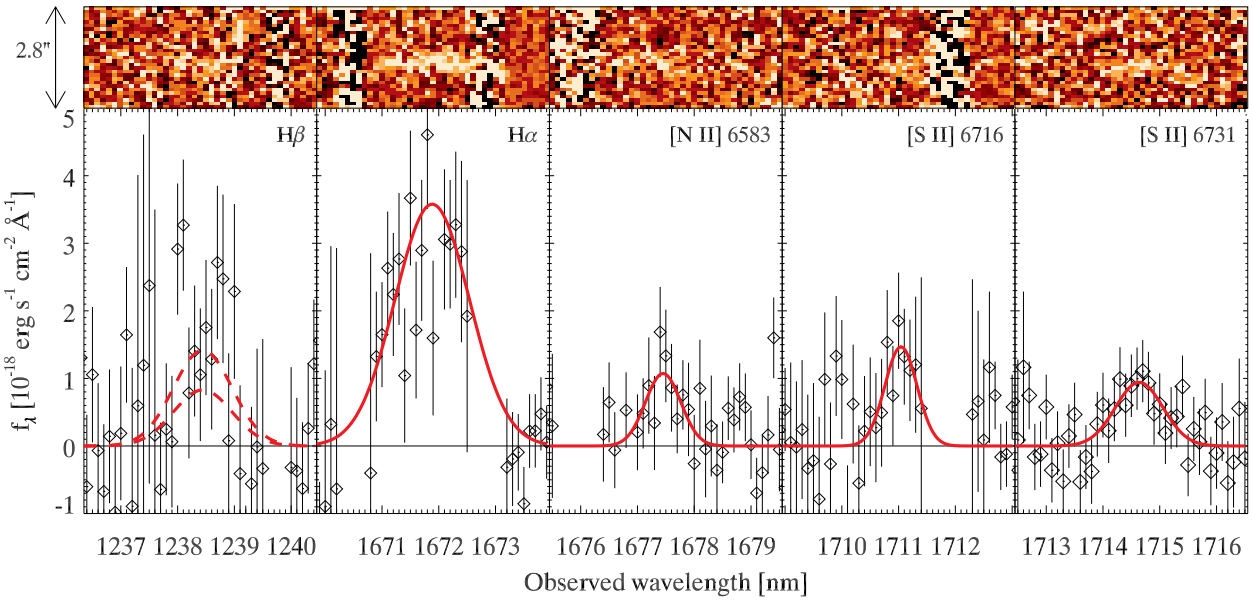

Fig. 2.— X-shooter 1D and 2D spectrum of hSDF0705.25. The spectrum has been corrected for Galactic extinction. The solid (red) line shows the fit to the emission lines assuming a Gaussian line profile. The dashed line shows a scaled version of the Hα line assuming the same FWHM (in velocity units) and extinction in the host of $E(B-V) = 0$ mag (upper) and $E(B-V) = 0.5$ mag (lower). Color version available online.

2.2. Spectroscopic data

The spectrum of hSDF0705.25 was obtained on 2012 April 23 with the X-shooter spectrograph (D'Odorico et al. 2006; Vernet et al. 2011) at the Very Large Telescope (VLT) at Cerro Paranal, Chile. We used an ABBA on-source nodding template with an exposure time of 1.3 hr (4×1200 sec) and a $0\farcs9$ slit[3]. The spectrum was obtained under clear conditions. For details on high-redshift emission-line spectroscopy with X-shooter see Frederiksen et al. (2012).

The X-shooter spectra were reduced using the official X-shooter pipeline[4] v1.3.7. The extraction of the object spectrum was conducted with our own IDL script, and flux calibration was done using the flux standard star, LTT 3218[5].

3. ANALYSIS

The flux-calibrated spectrum is corrected for Galactic extinction and slit loss. The Galactic extinction along the line of sight to hSDF0705.25 is $A_V = 0.042$ mag[6] (Schlafly & Finkbeiner 2011) and we assume the Galactic extinction law of Fitzpatrick (1999). The slit loss correction assumes a $\lambda^{-0.2}$ variation in seeing.

In the available atmospheric transmission windows, we detect a strong emission line at 1671.88 nm which we identify as Hα at $z = 1.54563 \pm 0.00027$. This identification is supported by the detection of Hβ, [N II] 6583, and [S II] 6716,6731 at the same redshift. We do not detect any continuum in the spectrum, only the strong emission lines in Figure 2. The detection of Hβ is severely affected by noise and therefore not fitted. We do not detect [O III] 4959,5007 in the spectrum and can therefore only derive upper limits on the flux. The detected emission lines in the corrected spectrum are fitted individually with a Gaussian line profile and the flux is calculated from the fit. The redshift is determined from the centroid of the fit to the individual lines (see Table 1). We apply a weighted average with weights equal to the inverse of the variance on the centroids, $w = \sigma^{-2}$. The derived redshift is consistent with the G11 photo-z value of $z = 1.552 \pm 0.018$.

---

[3]A $1\farcs0$ slit in the UVB arm.

[4]See, `http://www.eso.org/sci/software/pipelines/`

[5]See `http://www.eso.org/sci/observing/tools/standards/spectra/ltt3218.html`

[6]Quoted from the NASA/IPAC Extragalactic Database (NED) website: `http://ned.ipac.caltech.edu/`

We plot in Figure 2 a scaled-down version of the Hα line assuming case-B recombination, the same FWHM (in velocity units) and intrinsic reddening in the host of $E(B-V)$ of zero or 0.5 mag (Calzetti 2001) to illustrate the variation allowed by the spectrum.

The emission line ratios $N2 = \log([\mathrm{N\ II}]\,6583/\mathrm{H}\alpha)$ and $O3 = \log([\mathrm{O\ III}]\,5007/\mathrm{H}\beta)$ are among the main diagnostics for discriminating between star formation and AGN activity by way of the Baldwin, Phillips, & Terlevich (1981, BPT) diagram. The upper limit on $O3$ is calculated using the 3σ upper limit on [O III] and the predicted Hβ flux from the Hα flux. We calculate the Hβ flux assuming $E(B-V) = 0$ or 0.5 mag to make sure the classification does not depend on the assumed amount of extinction in the host galaxy. In both cases the host galaxy falls within the star-forming region of the BPT diagram (see Frederiksen et al. 2012, their Figure 5). The lack of a broad line component in the emission lines (see Table 1) also supports the conclusion that the line-flux is dominated by star formation and not AGN activity.

To constrain the metallicity of the host galaxy we make use of the emission-line ratios $N2$ and $N2O3 = \log([\mathrm{N\ II}]\,6583/[\mathrm{O\ III}]\,5007)$. Using the emission-line calibrations of Kewley & Dopita (2002), we apply a three-step iteration to set an upper limit on the metallicity. The first step involves using the $N2$ ratio to constrain the metallicity to either the upper or lower metallicity regime. The $N2$ ratio has the advantage of being virtually insensitive to extinction due to the close proximity of the two emission lines. The $N2$ ratio places the host galaxy in the low-metallicity regime at $12 + \log(O/H) < 8.55$. Next, we use the $N2O3$ ratio to refine the initial estimate. An upper limit on the [O III] line flux translates into a lower limit on $N2O3$. The lower limit on $N2O3$ places an upper limit on the ionization parameter $q < 2 \times 10^7$ cm s^{-1}, but due to the uncertainty in the intrinsic extinction of the host we take the precaution of placing the upper limit at $q < 4 \times 10^7$ cm s^{-1}, which would be consistent with $E(B-V) \sim 0.25$. Finally, we refine the metallicity estimate using the constraint on q. This gives us our final estimate of $12 + \log(O/H) < 8.0$. For comparison, the metallicity derived from the [N II]/Hα line ratio is 8.40 ± 0.18 (Pettini & Pagel 2004).

We convert the Hα flux to a rest-frame Hα luminosity and further into a star-formation rate (SFR) using the calibration of Kennicutt (1998), rescaled to a Chabrier (2003) initial mass function (IMF). The observed SFR, 4.0 ± 0.7 M$_\odot$ yr^{-1}, represents a lower limit to the intrinsic SFR of the host galaxy, due to the unconstrained extinction in the host galaxy.

The Photo-z fitter ZEBRA is not suited for deriving stellar parameters like the mass of the galaxy. We therefore fit the Subaru+UKIRT (B, V, R, i', z', J and K) photometric points (corrected for foreground extinction in the same way as the spectrum) using the FAST SED fitter (Kriek et al. 2009). We derive the intrinsic extinction, stellar mass and stellar age of the host galaxy (see Table 2). The extinction in the host is not very well constrained

($0 < A_V < 1.1$) so we assume $A_V = 0$ in our further analysis. We calculate the specific SFR, $sSFR$, using the Hα SFR and the stellar mass from FAST.

4. DISCUSSION AND CONCLUSIONS

Our derived spectroscopic redshift, $z = 1.54563 \pm 0.00027$, is in full agreement with the G11 photometric redshift of $z = 1.552 \pm 0.018$. We also exclude AGN activity as the source of the emission-line flux. From the flux of the Hα line we derive an observed SFR and from the emission line ratios we constrain the host-galaxy metallicity.

We find a highly star-forming (i.e., high sSFR), low-metallicity SN host galaxy (see Frederiksen et al. 2012, for the treatment of another high SF low metallicity SN host at similar redshift). The derived SFR is affected by extinction in the host galaxy, but due to the low signal-to-noise ratio of the Hβ line we are not able to place any strong constraints on it. Likewise the extinction derived from SED fitting does not provide a strong constraint.

The stellar mass and SFR place hSDF0705.25 midway between the $z = 1$ and $z = 2$ main-sequence of star-forming galaxies defined in Daddi et al. (2007) and Elbaz et al. (2007). As hSDF0705.25 falls within the main sequence at its redshift, it can be classified as an average star-forming galaxy at its redshift. Alternatively the specific SFR (sSFR) can be used to define whether a galaxy is a passive, a star forming or a star burst galaxy. Using the definition of Sullivan et al. (2006, $0.2 < z < 0.75$, see their Figure 6), the high sSFR of hSDF0705.25 makes it a star-burst galaxy.

Having two different measures of metallicity that do not agree is not unusual, as the absolute value of the metallicity depends on the calibration (also called the metallicity scale) used. Kewley & Ellison (2008) made the comparison between different metallicity calibrations and determined transformations to translate from one metallicity scale to another. From the transformation we expect PP04 to be systematically lower then KD02. The metallicity derived for this host galaxy is inconsistent with this tendency as the upper limit on the KD02 metallicity is $\sim 2\sigma$ lower then the PP04 metallicity. This is can be due to extinction effects or to some differences between theoretical and empirical calibrations that are not captured in KE04. The extinction effect is most important for the $N2O3$ line ratio (due to the wide separation between the lines). We have tried to account for extinction by assuming a conservative upper limit on $N2O3$ (assuming $E(B-V) = 0.25$). We therefore believe that the difference is due to differences between theoretical and empirical calibrations.

SNe Ia from low mass galaxies with high sSFR (and therefore low metallicity, see Lara-López et al. 2010; Mannucci et al. 2010, 2011) constitute the the bulk of the $z < 1$

Table 1. Spectroscopic summary

Line	Wavelength nm	Obs. FWHM[a] km s^{-1}	Int. FWHM[a] km s^{-1}	Flux 10^{-18} erg s^{-1} cm^{-2}
Hα	1671.88 ± 0.09	117 ± 18	103 ± 18	58.8 ± 10.4
[N II] 6583	1677.45 ± 0.07	47 ± 14	—	7.7 ± 3.1
[S II] 6716	1711.04 ± 0.11	50 ± 21	—	10.4 ± 5.0
[S II] 6731	1714.64 ± 0.09	73 ± 16	47 ± 16	9.9 ± 2.8
[O III] 5007[b]	—	—	—	< 23.2
[O III] 4959[b]	—	—	—	< 9.1

[a]The instrumental resolution is 57 km s^{-1}.

[b]This is the 3σ upper limit on the flux.

Table 2. Derived properties of SN host galaxy hSDF0705.25

Property	Value
Redshift	$z = 1.5456 \pm 0.0003$
Star-formation rate[ab]	$SFR = 4.0 \pm 0.7$ M$_\odot$ yr^{-1}
Metallicity (PP04)	$12 + \log(\mathrm{O/H}) = 8.4 \pm 0.2$
Metallicity (KD02)	$12 + \log(\mathrm{O/H}) < 8.0$
Ionization parameter (KD02)	$q < 4 \times 10^7$ cm s^{-1}
Stellar mass[c]	$\log(M_*[\mathrm{M}_\odot]) = 9.46^{+0.23}_{-0.08}$
Specific SFR	$\log(sSFR[\mathrm{yr}^{-1}]) = -8.86^{+0.11}_{-0.24}$
Host extinction[c]	$A_{V,\mathrm{host}} = 0.4^{+0.7}_{-0.4}$ mag
Stellar age[c]	$\log(t_*[\mathrm{yr}]) = 7.9^{+0.3}_{-0.6}$

[a]Assuming a Chabrier IMF.

[b]SFR is a lower limit as extinction in the host galaxy would make the intrinsic SFR higher.

[c]Using an exponentially declining star-formation history, redshift fixed to the spectroscopic redshift, and metallicity fixed to $Z = 0.008$ ($12 + \log(\mathrm{O/H}) \sim 8.4$).

SN Ia population (Sullivan et al. 2006, see). hSDF0705.25 is a similar low-metallicity, high-sSFR, host galaxy at $z = 1.55$ and therefore indicates the presence of such "prompt" SNe Ia also at these higher redshifts.

The SN Ia rates at high redshift are dominated by small-number statistics. The three $z > 1.4$ *HST*/GOODS SNe Ia belong to host galaxies with measured spectroscopic redshifts and no AGN activity. On the other hand, the larger Subaru/SDF sample includes ten SNe Ia at $z > 1.5$, but their classification as SNe Ia relies on photometric redshifts which, at high redshifts, might be systematically offset. Two ongoing *HST* Multi-Cycle Treasury programs, the Cluster Lensing and Supernova Survey with Hubble (Postman et al. 2012) and the Cosmic Assembly Near-IR Deep Extragalactic Legacy Survey (Grogin et al. 2011; Koekemoer et al. 2011) will find new SNe out to $z \approx 2.5$ (Rodney et al. 2012; Jones 2012), but their samples will still be small and will suffer from the same classification challenges faced by the GOODS and SDF surveys. It is thus imperative to test the robustness of the SDF SN Ia rate measurements by spectroscopically measuring the redshifts of the SN host galaxies (Frederiksen et al. 2012), and ascertaining whether the SN sample was contaminated by unclassified AGNs. The confirmation of the photometric redshift of hSDF0705.25, and its classification as a star-forming, non-AGN-hosting galaxy is the first step along this road.

Galaxy redshifts are usually measured either from bright emission lines or from the 4,000 Å break. Beyond redshift $z \sim 1.5$, the strong emission lines, like Hβ and [O III] 4959+ 5007, that we rely on to measure a galaxy's redshift are shifted into the near-IR and out of the wavelength range covered by most existing spectrographs, leaving only a single [O III] 3727 line in the optical window, with no other strong emission lines to confirm the redshift. The signal-to-noise of the [O III] 3727 line depends on the metallicity of the object, the amount of telluric absorption, and the atmospheric airglow lines present in the red part of the optical windows. Determining the redshift from the continuum requires prohibitively long exposure times. This is why $z \sim 1.5$ marks the start of the "redshift desert," where to date it has been exceedingly hard to measure galaxy redshifts. We have shown that X-shooter, with its uniquely long wavelength coverage from the near-UV to the near-IR, makes it possible to determine robust redshift measurements well into the "redshift desert" (see also Christensen 2011; Krühler et al. 2012). Yet this is still far from an easy task. hSDF0705.25 has been a test case and the first of the ten $z > 1.5$ SDF SN Ia host galaxies to receive a spectroscopic redshift. Of the remaining nine galaxies, three more can be targeted by X-shooter, two are too faint, and four are passive galaxies with no predicted emission lines. For these galaxies, the 4,000 Å break can only be targeted with the sensitivity of the *Hubble Space Telescope*.

We thank Martin Sparre for providing his X-shooter meta-pipeline, which has simplified the reduction of the X-shooter spectra significantly. The Dark Cosmology Centre is funded by

the Danish National Research Foundation. DM and OG acknowledge support by a grant from the Israel Science Foundation. This research has made use of the NASA/IPAC Extragalactic Database (NED) which is operated by the Jet Propulsion Laboratory, California Institute of Technology, under contract with the National Aeronautics and Space Administration.

Facilities: VLT:Kueyen (X-shooter), Subaru (SuprimeCam), GALEX, UKIRT (WFCAM)

REFERENCES

Baldwin, J. A., Phillips, M. M., & Terlevich, R. 1981, PASP, 93, 5

Benítez, N. 2000, ApJ, 536, 571

Bloom, J. S., et al. 2012, ApJ, 744, L17

Calzetti, D. 2001, PASP, 113, 1449

Chabrier, G. 2003, PASP, 115, 763

Christensen, L. 2011, Astronomische Nachrichten, 332, 301

Daddi, E., et al. 2007, ApJ, 670, 156

Dahlen, T., Strolger, L., & Riess, A. G. 2008, ApJ, 681, 462

Dahlen, T., et al. 2004, ApJ, 613, 189

Di Stefano, R., Voss, R., & Claeys, J. S. W. 2011, ApJ, 738, L1

D'Odorico, S., et al. 2006, in Society of Photo-Optical Instrumentation Engineers (SPIE) Conference Series, Vol. 6269, Society of Photo-Optical Instrumentation Engineers (SPIE) Conference Series

Elbaz, D., et al. 2007, A&A, 468, 33

Feldmann, R., et al. 2006, MNRAS, 372, 565

Fitzpatrick, E. L. 1999, PASP, 111, 63

Frederiksen, T. F., Hjorth, J., Maund, J. R., Rodney, S. A., Riess, A. G., Dahlen, T., & Mobasher, B. 2012, ApJ, in press, arXiv:1210.3053

Graur, O., & Maoz, D. 2012, ArXiv e-prints, arXiv:1209.0008

Graur, O., et al. 2011, MNRAS, 417, 916

Grogin, N. A., et al. 2011, ApJS, 197, 35

Hachisu, I., Kato, M., & Nomoto, K. 2012, ApJ, 756, L4

Hayashi, M., et al. 2009, ApJ, 691, 140

Howell, D. A. 2011, Nature Communications, 2

Iben, Jr., I., & Tutukov, A. V. 1984, ApJS, 54, 335

Jones, D. e. a. 2012, ApJ, in prep

Kashikawa, N., et al. 2004, PASJ, 56, 1011

Kennicutt, Jr., R. C. 1998, ARA&A, 36, 189

Kewley, L. J., & Dopita, M. A. 2002, ApJS, 142, 35

Kewley, L. J., & Ellison, S. L. 2008, ApJ, 681, 1183

Koekemoer, A. M., et al. 2011, ApJS, 197, 36

Kriek, M., van Dokkum, P. G., Labbé, I., Franx, M., Illingworth, G. D., Marchesini, D., & Quadri, R. F. 2009, ApJ, 700, 221

Krühler, T., et al. 2012, ApJ, 758, 46

Lara-López, M. A., et al. 2010, A&A, 521, L53+

Leibundgut, B. 2000, A&A Rev., 10, 179

Ly, C., et al. 2009, ApJ, 697, 1410

Mannucci, F., Cresci, G., Maiolino, R., Marconi, A., & Gnerucci, A. 2010, MNRAS, 408, 2115

Mannucci, F., Salvaterra, R., & Campisi, M. A. 2011, MNRAS, 414, 1263

Maoz, D., & Mannucci, F. 2012, PASA, 29, 447

Maoz, D., Mannucci, F., & Brandt, T. D. 2012, ArXiv e-prints, arXiv:1206.0465

Nomoto, K. 1982, ApJ, 253, 798

Nugent, P. E., et al. 2011, Nature, 480, 344

Perrett, K., et al. 2012, AJ, 144, 59

Pettini, M., & Pagel, B. E. J. 2004, MNRAS, 348, L59

Postman, M., et al. 2012, ApJS, 199, 25

Riess, A. G., et al. 2004, ApJ, 607, 665

Rodney, S. A., et al. 2012, ApJ, 746, 5

Schlafly, E. F., & Finkbeiner, D. P. 2011, ApJ, 737, 103

Strolger, L., Dahlen, T., & Riess, A. G. 2010, ApJ, 713, 32

Strolger, L., et al. 2004, ApJ, 613, 200

Sullivan, M., et al. 2006, ApJ, 648, 868

Vernet, J., et al. 2011, A&A, 536, A105

Webbink, R. F. 1984, ApJ, 277, 355

Whelan, J., & Iben, Jr., I. 1973, ApJ, 186, 1007